CHAPTER IV
MICROWAVE DIELECTRIC PROPERTIES OF THE POLYBENZOXAZINE BASED/BST COMPOSITES

4.1 Abstract

The polymer-ceramic composites are the developed materials for the microelectronic device which are interested in recent years. High dielectric constant (ε_r) and low loss tangent (tanδ) are the significant requirement for microwave substrate application. In this work, At 1 GHz, aniline based benzoxazine monomer showed the higher dielectric constant than the fluorine based benzoxazine monomer (6.12 and 4.49, respectively). In case of loss tangent, both of benzoxazine based monomer given the loss tangent value less than 0.03 which stay in feasible range for high frequency application. Then, the microwave dielectric properties of the composites between PBA-a and Barium strontium titanate, $Ba_{1-x}Sr_xTiO_3$, (BST) fillers were studied as a function of the ceramic content. The higher ceramic content was related to the higher dielectric constant and loss tangent (ε_r = 21.94 and tan δ = 0.0054, by adding 80 wt%). The frequency dependent dielectric was found that, at higher frequency (100 MHz- 1 GHz) the dipole orientation polarization start inactive so the total polarization of the composite decrease. The higher loss tangent was observed because the effect of the agglomerate of ceramic filler. In addition, the temperature dependent dielectric constant of the composites were observed at 1 MHz to 100 MHz because of the decrease of molecule alignment while high loss tangent was observed at 1 GHz which was attributed to the segregation of the polymer chain and void creation.

Keyword: Polybenzoxazine, barium strontium titanate, microwave dielectric properties

4.2 Introduction

The increasing consumption of microelectronic devices and telecommunication has been interest in recent year. The passive electronic devices require high performance with enhance reliability, lower cost, lower size and weight that are significant efforts in research and development. The polymer-ceramic composite is the new material which has optimum properties for electronic application, because ceramic has high own dielectric properties but it is difficult processed while polymer often is low cost and easily to process which can increase the relaxation phenomena and dielectric losses. Ferroelectric materials with optimal dielectric constants and dissipation factors have received considerable attention, since their growing use in various electronic devices. Especially, nowadays the microelectronics devices usually made from ferroelectric ceramic–polymer composites. These materials are good candidates for embedded capacitors, capacitively coupled electrical solutions and other integrated high-frequency electronic devices. Ferroelectric ceramic–polymer composites made of barium strontium titanates $Ba_{1-x}Sr_xTiO_3$ (BST) with different polymers, such as epoxy, polyvinylidene fluoride (PVDF), polyimide, cyanoethylated cellulose polymer, etc., have been investigated for microwave substrate application [1-3].

Polybenzoxazine is the new member in the family of phenolic resins which have not only the characteristics of traditional phenolic resins such as excellent thermal properties and flame retardance but also unique characteristics such as molecular design flexibility, low moisture absorption, near zero shrinkage upon polymerization, low melt viscosity, low coefficient of thermal expansion (CTE) and good dielectric properties. Thus, polybenzoxazine overcome the disadvantages of the traditional phenolic resins, which lead to a novel and promising candidate for high performance thermosetting resins [4-5] that usually used as polymer matrix in electronic application.

The main objective of this research was to improve the dielectric properties of the polybenzoxazine composite with different loading of BST for applications at microwave frequency. The effect of volume of BST ceramics on the frequency and temperature dependent dielectric properties of composites were studied. In this work,

the benzoxazine monomers were synthesized by either aniline based or fluorinate based monomers. BST powders were prepared from the sol-gel method. Subsequently the dielectric properties of composite were measured at microwave frequencies (1MHz - 1GHz).

4.3 Experimental

4.3.1 Synthesis of Aniline Based Benzoxazine Monomer

The preparation of aniline based benzoxazine monomer is based on the reaction of bisphenol A, paraformaldehyde and aniline at the molar ratio of 1:4:2 respectively as shown in Figure 4.1 and for this experiment, the monomer was prepare by solventless method .The starting materials were mixed together without solvent at temperature of 100°C for 30 min. Then the product with high yellow viscous liquid was obtained. This viscous product was dissolved in chloroform and washed sequentially with 0.1 N Sodium hydroxide (NaOH) and water for 3 times to eliminate any unreacted formaldehyde and dried over sodium sulfate (Na_2SO_4). Then the chloroform was used to remove with a rotary evaporation and the solid products were washed by cool methyl alcohol at least 3 times to obtain the white powder benzoxazine monomer.

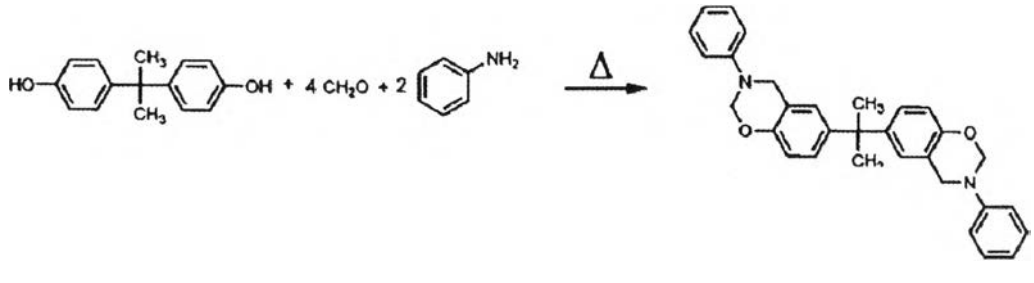

Figure 4.1 Synthesis of aniline-based benzoxazine (Ghosh *et al.*, 2007).

4.3.2 Synthesis of Fluorinate Based Benzoxazine Monomer

The same procedure as aniline based monomer to prepare the fluorinate based benzoxazine monomer was followed. The starting chemicals, hexafluorobisphenol A, paraformaldehyde, and aniline were prepared at molar ratio of 1:4:2, as shown in Figure 4.2.

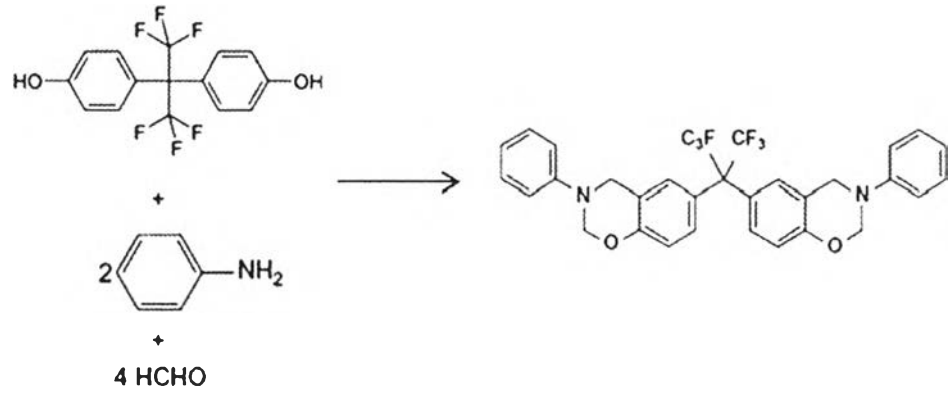

Figure 4.2 Synthesis of fluorinate-based benzoxazine (Su *et al.*, 2003).

4.3.3 Preparation of Barium Strontium Titanate by Sol-Gel Process

Barium strontium titanate ($Ba_{0.3}Sr_{0.7}TiO_3$) was prepared by dissolving 0.3 mole of barium acetate and 0.7 mole of strontium acetate separately in acetic acid, followed by the addition of methyl alcohol to each one. The solution were then mixed and stirred to obtain a clear solution. Then an equimolar amount of titanium n-butoxide was added into this mixture under vigorous stirring. When the solution became a gel, it was calcined by using 2-step thermal decomposition to decompose the solvent and crystallize $Ba_{0.3}Sr_{0.7}TiO_3$ powders are shown in Figure 4.3.

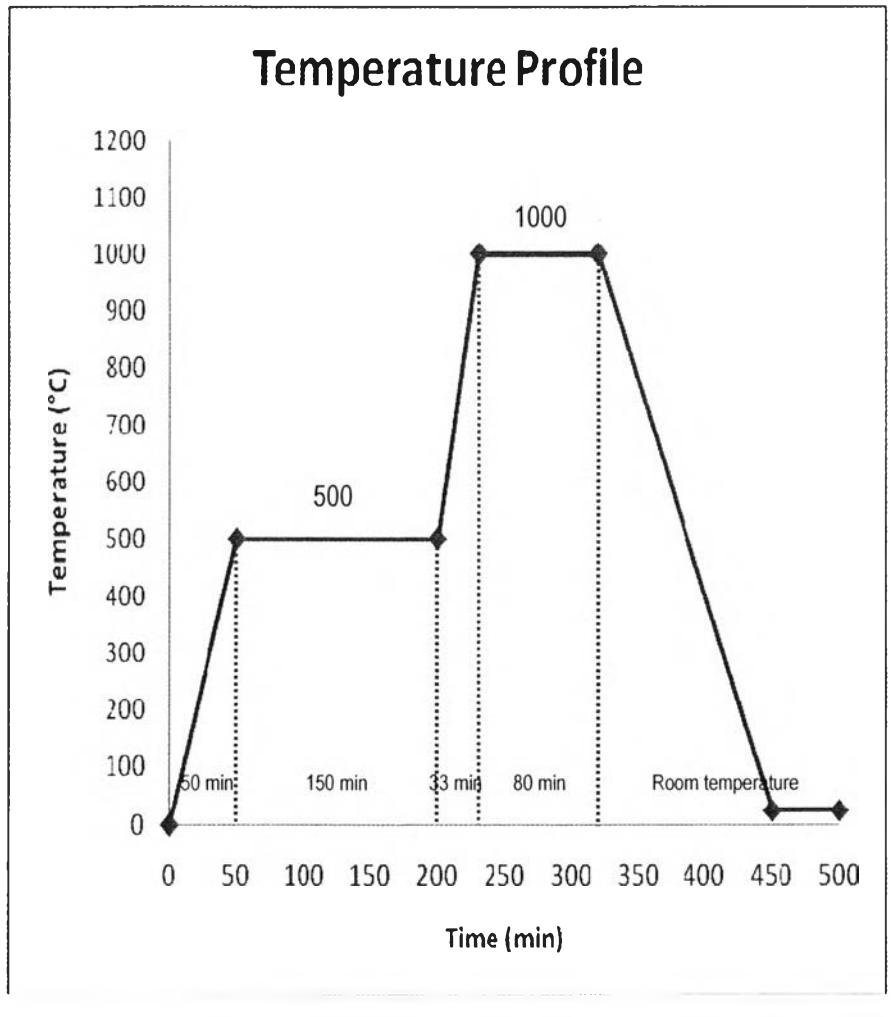

Figure 4.3 The Temperature profile for two-step thermal decomposition of BST.

4.3.4 Composite Preparation

The composite between polybenzoxazine based and BST ceramic ($Ba_{0.3}Sr_{0.7}TiO_3$) were prepared. Owing to the much difference between the densities of 2 substrate, mixing of the benzoxazine monomer and BST powder with 30, 40, 50, 60, 70 and 80 wt% by melt mixing process was applied to prevent the separation of 2 phases. Later, the mixtures was fabricated as composite specimens with the thickness of 1.2 mm. and 2.0 mm in diameter by compression molding with curing conditions were given in Table 4.1.

Table 4.1 Temperature profile for compression molding process

Temperature (^{o}C)	Time (minute)	Applied load (150 kg.)
120	30	-
140	30	-
160	30	-
180	30	-
200	30	+
230	60	+

4.3.5 Characterizations and testing

The chemical structures of the benzoxazine based monomers were confirmed by Nuclear Magnetic Resonance Spectrometer (Bruker Avance DPS-400, NMR) and Fourier Transformation Infrared Spectroscopy (NEXUS 670, FTIR) spectrometer. The heating profile of benzoxazine monomer was performed by a differential scanning calorimeter 7, DSC 7 (Perkin Elmer). A crystal phase and structure of BST powders was analyzed by X-ray differaction (Rigaku, model Dmax 2002) while the particles size of sol-gel BST powders was observed by transmission electron microscope (TEM; H-7650, Hitachi). The apparent density of BST powders and benzoxazine monomer were measured by pycnometer (Quantachrome, Ultrapycnometer 1000) under helium purge at pressure of 20 psi. Glass transition temperature (Tg) of polybenzoxazine was measured by GABO EPLEXOR 100 N operated at 1 Hz under N_2 with flow rate of 100 ml/min. The thermal stability properties of the composite was measured by Perkin Elmer Pyris Diamond TG/DTA instrument by using the platinum pan for reference and operated the heat from 30 °C to 900°C and heating rate of 10°C/mins. This condition is flow under N_2 with flow rate of 100 ml/min. For microwave dielectric properties of the composites were measured at -50 to 150°C for temperature dependant and at frequency range of 1MHz – 1GHz for frequency dependence by Agilent E4991A RF Impedance/Material Analyzer (Agilent Technologies Inc., USA). Microstructure and surface morphology of BST powders and the composite were observed by a scanning electron microscope (SEM; HITACHI S-4800) at voltage of 15 kV. Moreover, the microstructure and surface morphology of BST powders and the composite were observed by a scanning electron microscope (SEM; HITACHI S-4800) at voltage of 15 kV.

4.4 Results and Discussions

4.4.1 Benzoxazine Monomers and Polymers Characterization

Aniline based benzoxazine monomer (BA-a) and fluorine based benzoxazine monomer (BA-f) that were synthesized from solventless method were characterized by using FTIR spectrometer to investigate the functional groups. The FTIR spectrums of BA-a monomer and BA-f monomer are shown in Figure 4.4 and 4.5, respectively.

The FTIR spectrums show the tri-substituted benzene ring mode in oxazine ring structure at 1496 cm^{-1} for BA-a monomer and at 1499 cm^{-1} for BA-f monomer. The antisymmetric C-N-C stretching mode can be indicated in the absorption band around 1240-1020 cm^{-1} whereas the symmetric mode appears at 830-740 cm^{-1}. The band around 1240-1210 cm^{-1} and 1040-1020 cm^{-1} indicate the antisymmetric and symmetric C-O-C stretching modes, respectively. Moreover, the band between 960 and 920 cm^{-1} attributes to the benzene with an attached oxazine ring modes [6]. For BA-f monomer, the C-F characteristic absorption bands are shown at 1200-1100 cm^{-1}. Lastly, the purification of the synthesized BA-a monomer and BA-f monomer are confirmed by the absence of band around 3600-3200 cm^{-1} which are the peaks of intermolecular hydrogen boned group [7].

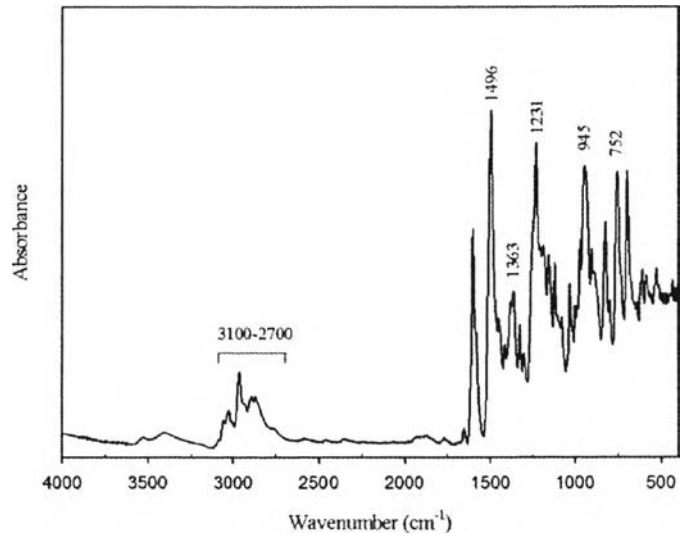

Figure 4.4 FTIR spectra of aniline based benzoxazine monomer (BA-a).

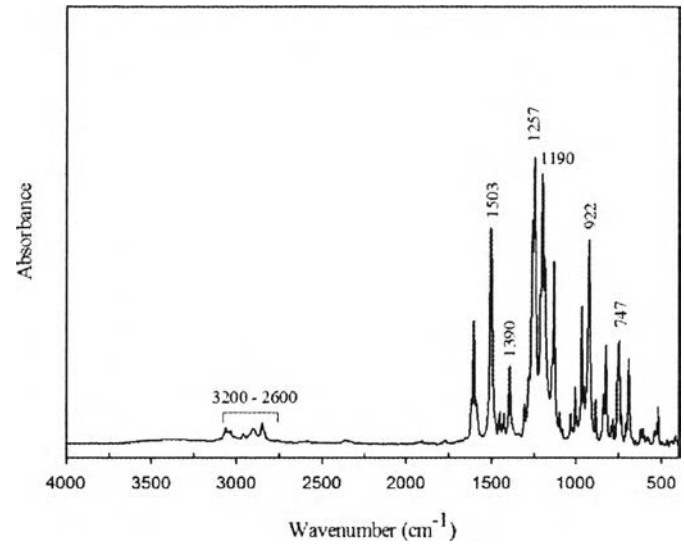

Figure 4.5 FTIR spectra of fluorine based benzoxazine monomer (BA-f).

^{1}H NMR spectra was used to indicate the chemical structure of BA-a monomer and BA-f monomer as shown in Figure 4.6 and 4.7, respectively. And ^{19}F NMR spectra also used for BA-f monomer are shown in Figure 4.8.

For BA-a monomer, the characteristic peak of aromatic proton displayed multiplets peak at around 6.7-7.3 ppm. The methylene (O-CH_2-N) and methylene (Ar-CH_2-N) of oxazine ring indicated peaks at 5.35 and 4.6, respectively. In addition, the NMR spectra of methyl proton of bisphenol A (-CH_3) was observed at 1.6 ppm. Meanwhile, the peak of aromatic proton, O-CH_2-N and Ar-CH_2-N of BA-f monomer showed spectra at 6.8-7.3, 5.4and 4.6 ppm, respectively (Ishida et al., 1995). And the peak of C-CF_3 which was observed by ^{19}F NMR spectra showed at -64.9 to -65.05 ppm. The formation of fluorinate benzoxazine ring was confirmed by the slight of chemical shift within 1 ppm. The purification of both monomers was indicated from ^{1}H NMR spectra which no peaks of methylene groups from the oligomers (oxazine ring-opening process) at 3.10 and 3.60 ppm [8].

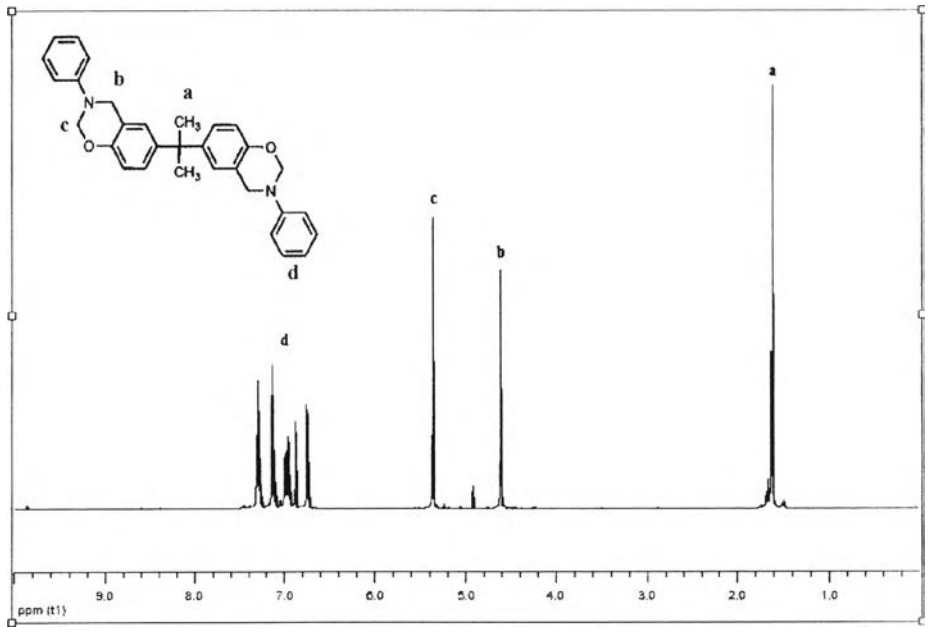

Figure 4.6 ^{1}H-NMR spectra of the aniline based benzoxazine monomer (BA-a).

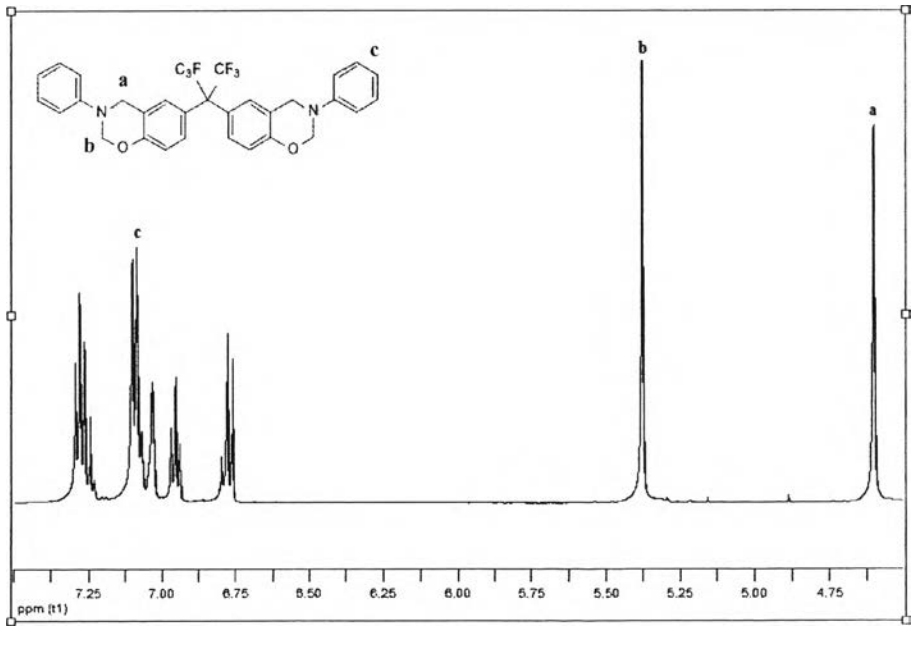

Figure 4.7 ^{1}H-NMR spectra of the fluorine based benzoxazine monomer (BA-f).

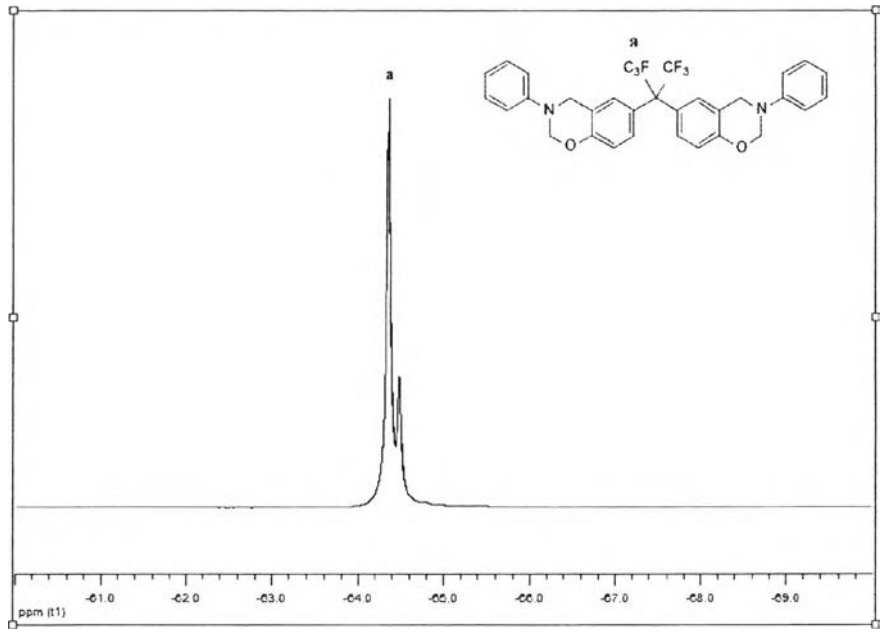

Figure 4.8 ^{19}F-NMR spectra of the fluorine based benzoxazine monomer (BA-f).

The DSC thermogram in Figure 4.9 shows the peak maximum and the exotherm onset at 231.80°C and 218.09°C, respectively for BA-a monomer. This graph refers to the reaction of ring opening polymerization that was occurred at 218.09°C by heat. While the DSC peak of BA-f monomer appears the melting endotherm peak at 190.83°C which nearly curing exotherm peak at 227.59°C. This indicates that the crosslink reaction occurs immediately after monomers start to polymerization.

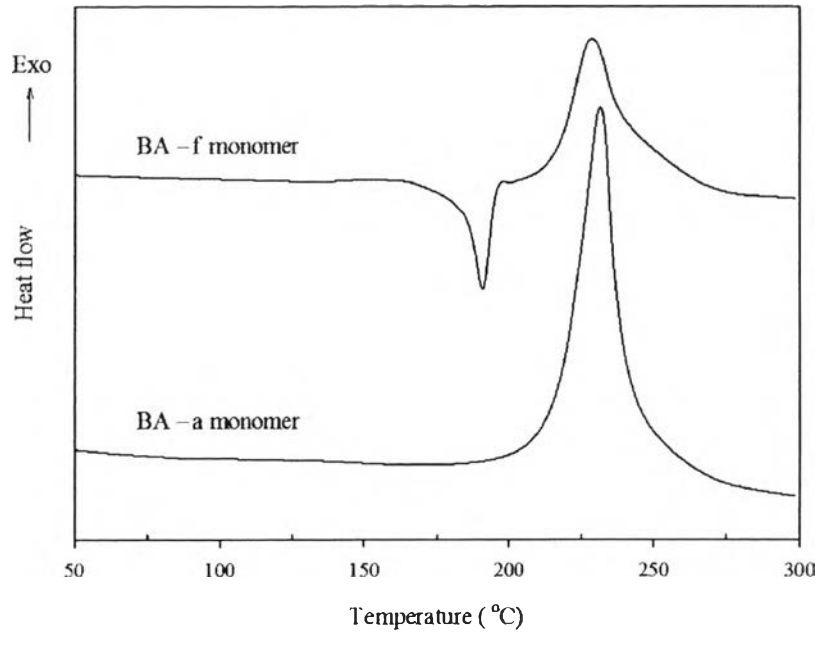

Figure 4.9 DSC thermogram of BA-a monomer and BA-f monomer.

4.4.2 Microwave Dielectric Properties of Polybenzoxazine Based

4.4.2.1Frequency Dependent Dielectric properties

In Figure 4.10, it shows the dielectric constant (ε_r) of the PBA-a and PBA-f at 1MHz – 1GHz as a function of frequency dependence. The slightly decrease in dielectric constant with frequency increase was observed in both of polybenzoxazine. At the same frequency, the dielectric constant of PBA-a was higher than PBA-f for example, at 1GHz, the dielectric constant of PBA-a PBA-f were 6.12 and 4.49, respectively because the decreasing of dipole orientation polarizability in the polymer molecule. Dipole orientation polarizability was too slow to completely follow the oscillation of the applied electric field when the frequency of applied electric field was above the relaxation frequency so; the contribution from this polarization mechanism was reduced. There are three reasons which were explained in term of chemical structure. For the lower of dielectric constant of BA-f: (1) the strong electron-withdrawing group,–CF_3 group, of PBA-f show the inductive effect and decreases the electronic polarizability; (2) the decreasing of molecular packing efficiency due to bulky –CF_3 group lead to increase the free volume (ε_r of air near

zero); (3) the lower polarizability of C–F bond can induce the hydrophobicity of the polymer. Because the moisture has a very high dielectric constant, it strongly affects the dielectric constant of the polymer (ε_r of water = 78.5 at 25°C)[9]. While, the loss tangent of the polybenzoxazine based stayed within feasible range (lower than 0.03) so it can neglect as shown in Figure 4.11.

4.4.2.2 Temperature Dependent Dielectric Properties

The temperature dependent dielectric constant and loss tangent of both polybenzoxazine from -50°C-150°C was shown in Figure 4.12 and 4.13, respectively.

At 1GHz and temperature range of -50°C to 140°C of PBA-a, the dielectric constant showed constant value but significant decreased at 150°C which is contributed from the lower orientation polarization when the temperature increase while, PBA-f (1 GHz), the dielectric constant was increased with temperature due to at high temperature the segmental mobility of polymers was increased that result to the dipole orientation mode of polarization was dominant. Loss tangent of both PBA-a and PBA-f was independence to temperatures. While the other frequencies (1M, 10M and 100M) also exhibit the same behavior. From all above results, PBA-a was chosen to use as a polymer matrix of the composite [10].

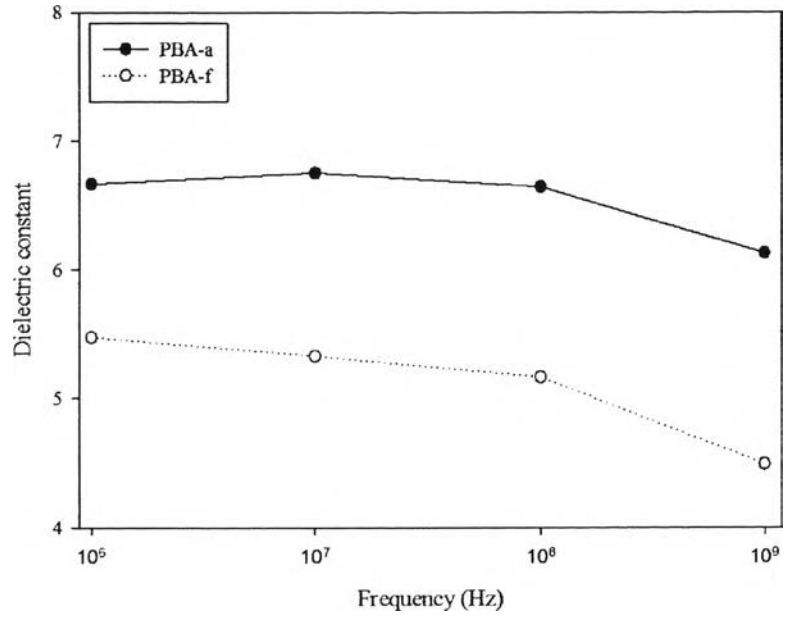

Figure 4.10 The frequency dependence of dielectric constant (ε_r) for polybenzoxazine at 1MHz – 1GHz.

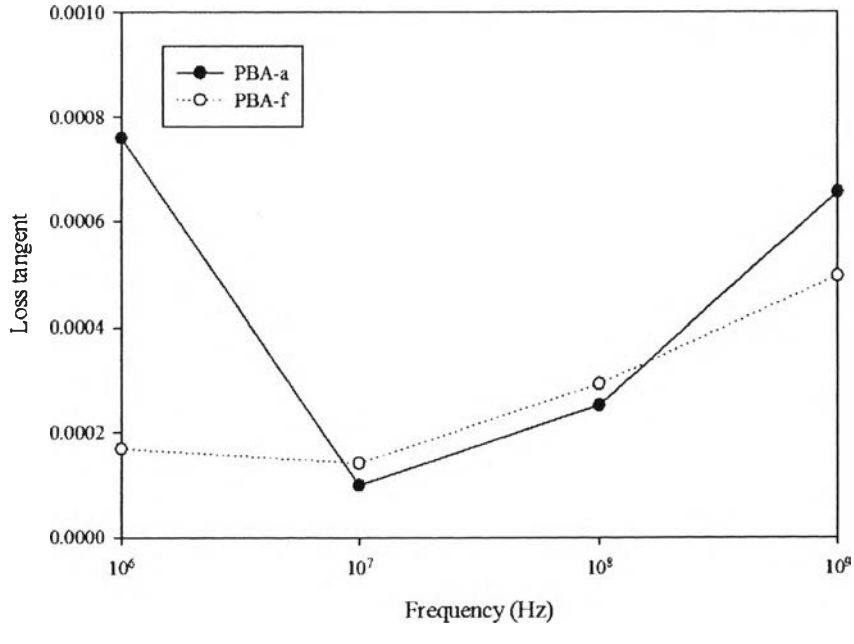

Figure 4.11 The frequency dependent loss tangent (tan δ) of the polybenzoxazine at 1MHz – 1GHz.

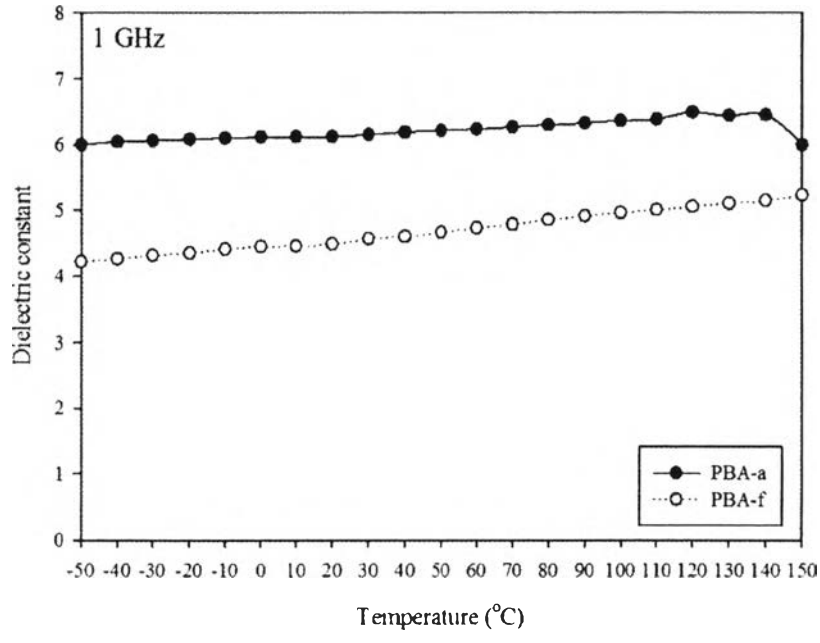

Figure. 4.12 The temperature dependence of dielectric constant (a) for polybenzoxazine at 1 GHz and -50°C to 150°C.

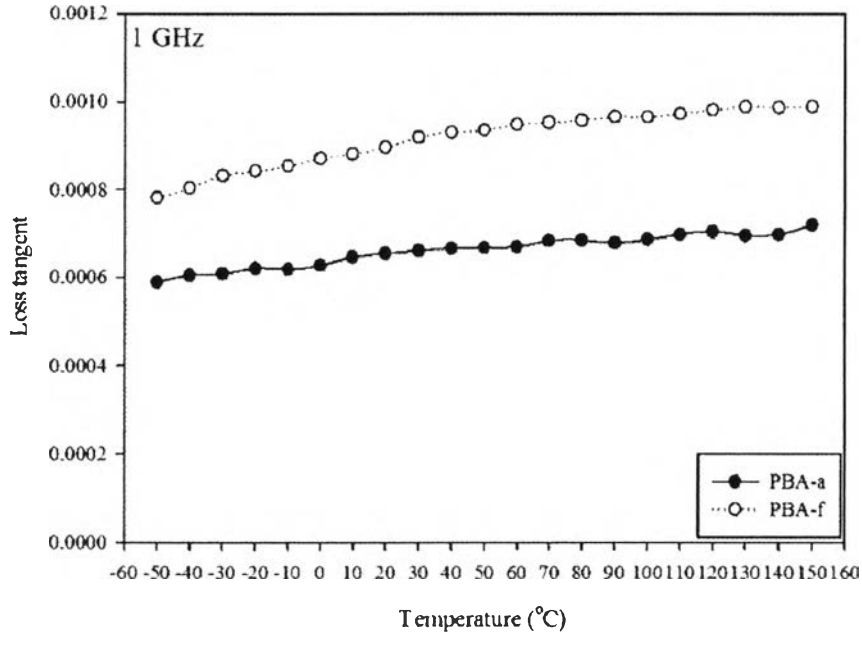

Figure. 4.13 The temperature dependence of loss tangent for polybenzoxazine at -1 GHz and 50°C to 150°C.

4.4.3 Barium Strontium Titanate ($Ba_{0.3}Sr_{0.7}TiO_3$) Characterization

The crystal structure of the sol-gel barium strontium titanate (BST) powder was confirmed by the X-ray diffraction (XRD) in Figure 4.14. The XRD patterns indicates the reflection peaks at 2θ values of 22.6°, 32.2°, 39.8 °, 46.1 °, 51.95 °, 57.59 ° and 67.39 ° corresponding to (100), (110), (111), (200), (210), (211) and (220) set of diffraction planes, respectively. These results show that after the calcinations process, the structure of BST gel transformed to the perovskite structure. Moreover, the cubic structure of BST particle was confirmed by the absence of peak splitting at 2θ =46.1° [11].

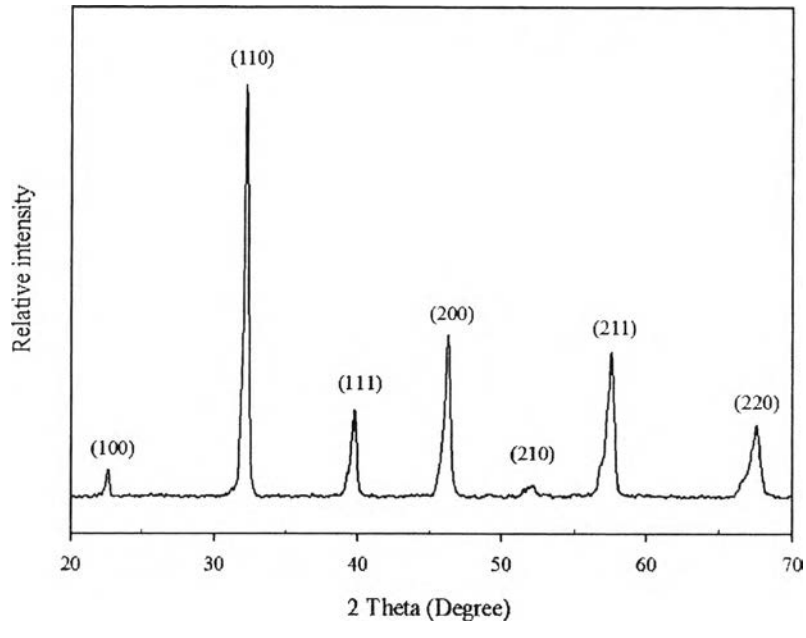

Figure 4.14 X-ray diffraction pattern of sol-gel BST powder.

FTIR spectrophotometer also used to confirm the functional groups of sol-gel BST powder. In Figure 4.15, IR spectrum peak was observed at 557 cm^{-1} which is the effect of Ti-O stretching vibration of TiO_6 octahedron[2].

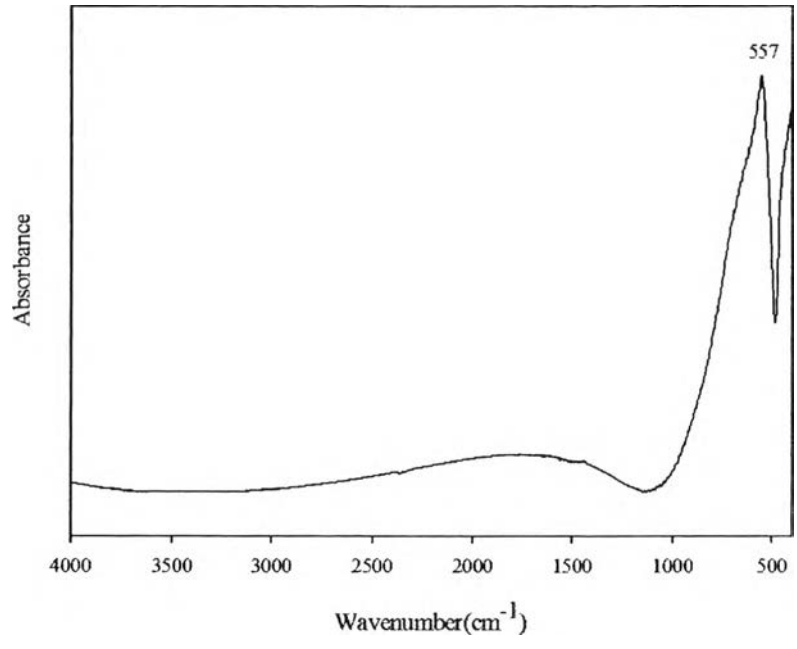

Figure 4.15 FTIR spectra of sol-gel BST powder.

As indicated in TEM image, Figure 4.16, the morphology of the BST powder which was prepared by sol-gel method shows the particle mostly agglomerate and uniformly particle size and shape distribution furthermore, it were a spherical shape with average size around 40-60 nanometers in diameter.

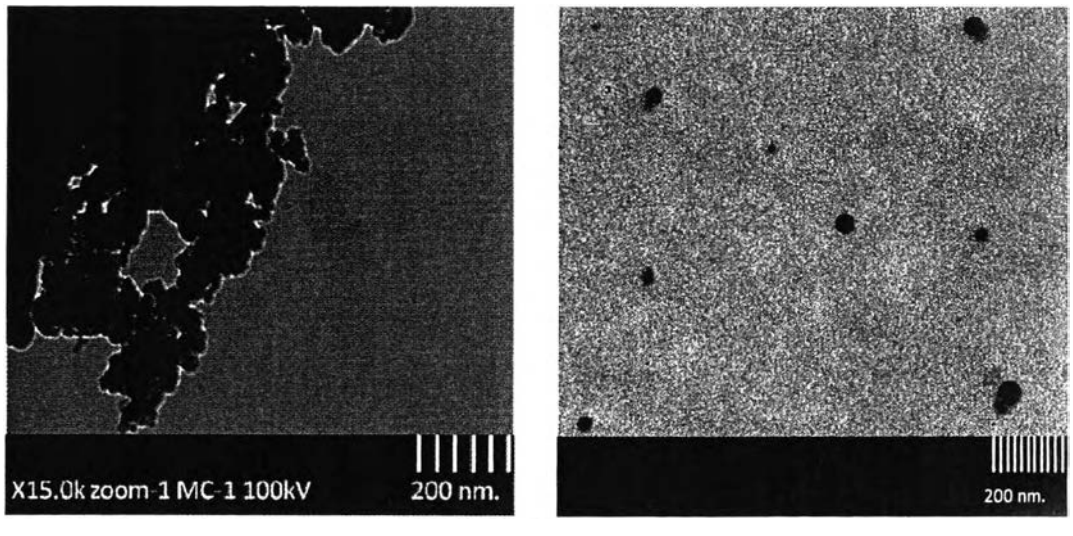

Figure 4.16 TEM image of sol-gel BST powder.

4.4.4 PBA-a/Barium Strontium Titanate Composites Characterization

4.4.4.1 Thermal Gravimetric Analysis (TGA)

Thermal stability and thermal properties of the pure PBA-a and the composite which consist of BST filler in 30, 40, 50, 60, 70 and 80 wt% measure by TGA in nitrogen atmosphere is shown in Figure 4.17 and Table 4.2. TGA curve of the pure PBA-a shows that there is 3.24 % residual weight up to 900 °C. Meanwhile, the residual weights of the composites increase with the amount of BST loading (up to 80.4 %). This can confirm that the existence of BST ceramic filler can improve the thermal stability of the composites. The increasing of the decomposition temperature was attributed to the enhancement of the interaction between polymer and ceramic phase implied that the movement of the polybenzoxazine was limited.

Table 4.2 Thermal properties of PBA-a/BST composites

Materials	BST Volume fraction	T_{d10} (°C)	Residual weight (%) at 900°C
Pure PBA-a	0.00	215.2	3.24
PBA-a/BST 30 wt%	0.09	327.1	47.3
PBA-a/BST 40 wt%	0.13	335.7	55.8
PBA-a/BST 50 wt%	0.18	349.1	62.5
PBA-a/BST 60 wt%	0.25	351.9	71.8
PBA-a/BST 70 wt%	0.34	364.8	76.1
PBA-a/BST 80 wt%	0.49	392.4	80.4

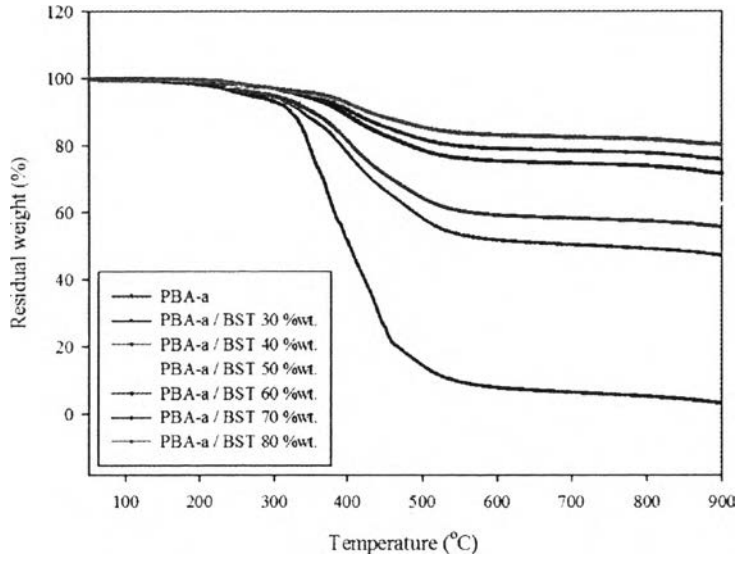

Figure 4.17 Thermal Gravimetric Analysis (TGA) curve of pure PBA-a and PBA-a/BST composites.

4.4.4.2 Dynamic Mechanical Analysis (DMA)

The dynamic mechanical spectra of aniline based polybenzoxazine and the PBA-a/BST composite (from 30 wt% to 80 wt %) are presented in Figures 4.18.

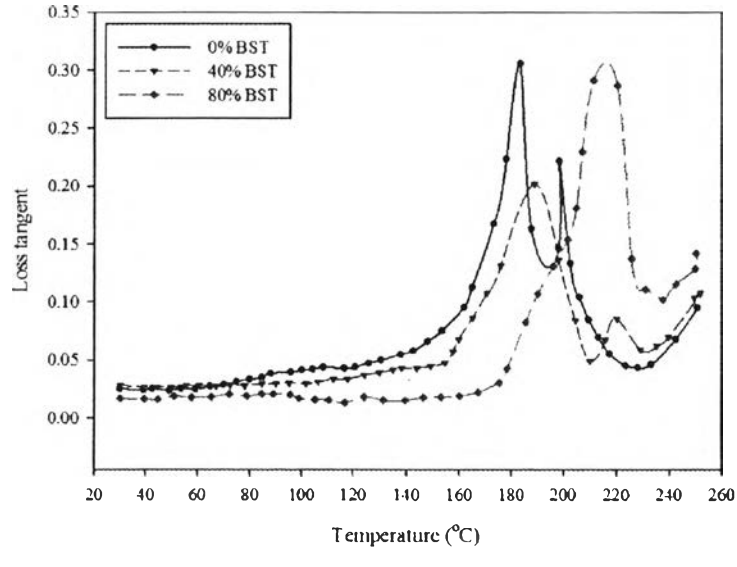

Figure 4.18 Loss tangent of PBA-a/BST composites at various BST contents.

The loss tangent which showed on the DMA thermograms revealed the glass transition temperature. At higher BST ceramic content, glass transition temperature (T_g) shifted to higher temperature due to the enhancement of rigid phase (BST ceramic phase). Furthermore, the area under the loss tangent graph related to the dissipate energy of the materials. The larger area of the composite with 80 wt% BST referred to higher of the rigid region (BST filler). Because the rigid region can dissipate energy more than the flexural phase (polymer chain). For the storage modulus are illustrated in Figure 4.19, the thermograms revealed the glassy state moduli. At 30 °C, It reported the storage modulus of PBA-a as around 5.2 GPa while, the composite with 80 wt% BST to be approximately 5.7 GPa. These result can refer to the BST is much more stiff than the PBA-a owing to the molecule structure of polymer is more flexible than ceramic structure. The temperature drop on the graph can explain about the temperature of the materials that used for change the state. The composite with BST 80 wt% indicated the higher temperature than composite with 40 wt% and pure polymer which mean the mechanical stiffness properties of the composites were improved by ceramic filler content [12].

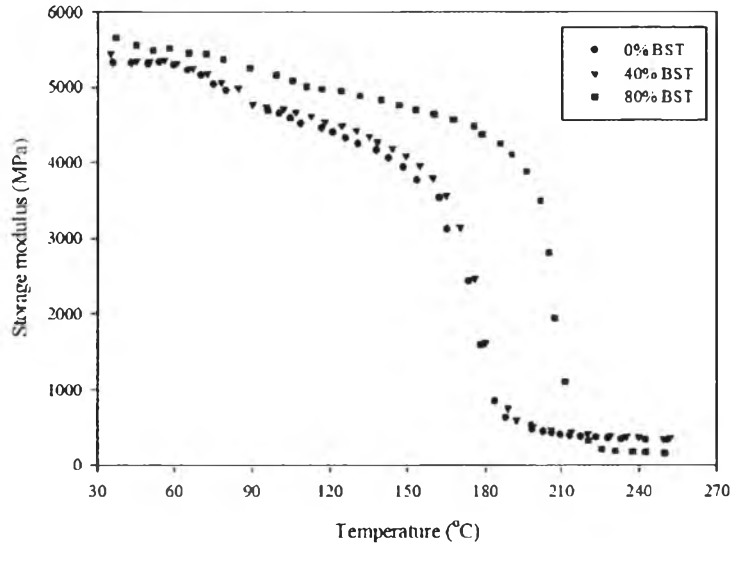

Figure 4.19 Storage modulus of PBA-a/BST composites at various BST contents.

4.4.4.3 Density Measurement

The density of the polybenzoxazine based (PBA-a), calcined BST powder and the composites at various BST content was measured by pyconometer. Theoritical density of material was calculated by using equation (5.1):

$$\rho_T = (1 - \emptyset)\rho_p + V\rho_c \quad (4.1)$$

where ρ_c is the ceramic filler density, ρ_p is the polymer matrix density and $\emptyset$ is the volume fraction of ceramic filler. Density of PBA-a and calcined BST powder is 1.27 and 5.19 g/cm^3, respectively. In Table 4.3, the densities of the PBA-a/BST composites with vasious BST content are summarized. Moreover, the experimental density can fit well with the theoretical density at the variation of BST content in the composite as shown in Figure 4.20.

Table 4.3 Densities of the composite at various contents

Materials	Volume fraction	Density (g/cm^3)
Pure PBA-a	0.0000	1.17
PBA-a/BST 30 wt%	0.00875	1.23
PBA-a/BST 40 wt%	0.1297	1.57
PBA-a/BST 50 wt%	0.1828	1.80
PBA-a/BST 60 wt%	0.2512	1.96
PBA-a/BST 70 wt%	0.3429	2.34
PBA-a/BST 80 wt%	0.4876	2.80
Pure BST	1.000	5.75

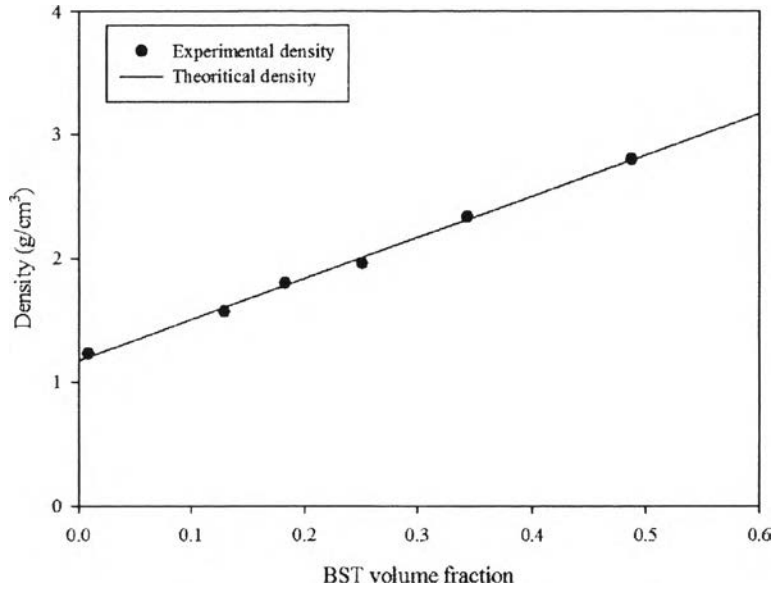

Figure 4.20 The comparison between (•) experimental and (-) theoretical density as a function of BST volume fraction.

4.4.4.4 Ceramic Filler Distribution

The distribution of the BST filler in the PBA-a matrix was invertigated by SEM micrographs. Figure 4.21 (a)-(f) show the surface morphology of the composites with the BST of 30, 40, 50, 60, 70 and 80 wt%, respectively. The white and gray colors represent the BST filler and black color represents the PBA-a matrix respectively. From the SEM images, it showed that the dispersion of BST powder was not uniform even in the lowest BST content. The BST filler tended to form larger size when the BST contents were higher which might be the effect of the van der waal force.

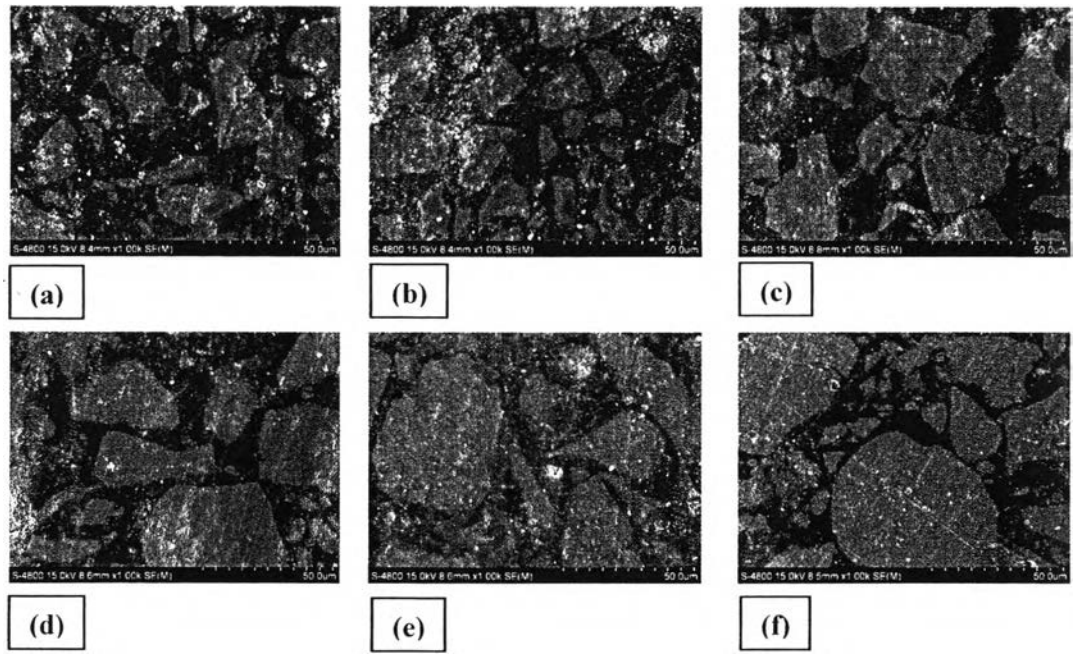

Figure 4.21 SEM micrographs of the surface morphology of the composites loading (a) 30 wt% (b) 40 wt% (c) 50 wt% (d) 60 wt% (e) 70 wt% and (f) 80 wt%.

4.4.5 Microwave dielectric properties of PBA-a/BST composites

4.4.5.1 BST filler concentration effect

The dielectric constant and loss tangent of the composite with various BST contents as a function of ceramic volume fraction, from 1 MHz to 1 GHz are shown in Figure 4.22 and 4.23, respectively. As can seen in Figure 4.24, it was found that at the same frequency, the dielectric constant o the PBA-a/BST composites increased with the ceramic volume fraction increase owing to at higher ceramic volume fraction, the ceramic come closer together then the interfacial area between the ceramic and polymer phase increase, the dipole -dipole interaction increase and contribute to the higher dielectric constant. Generally, the loss tangent of composites also increases with the ceramic volume fraction as shown in Figure 4.23. From the results, the dielectric constant of the composites at 1 GHz increased from 6.12 to 22 as the volume fraction of BST was increased from 1.17 to 48.7 vol.%, about 3 times of pure PBA-a. While at 1 GHz, loss tangent of the composites increased from 0.0011 to 0.0054 which also stay in acceptable range[3].

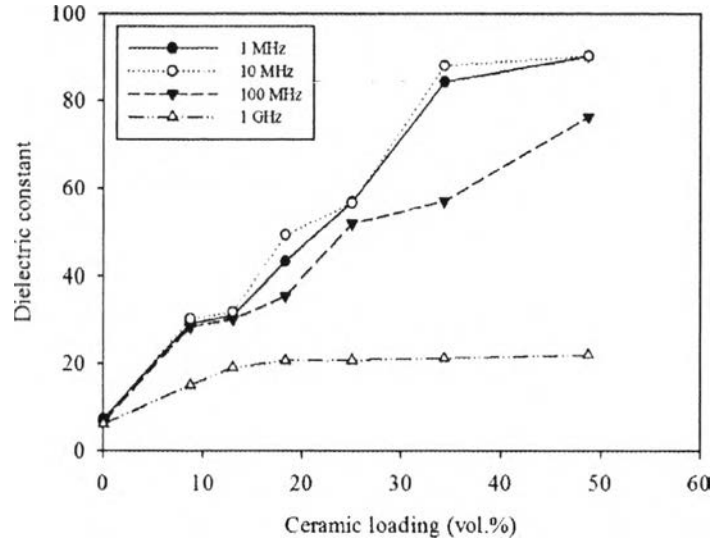

Figure 4.22 Dielectric constant of the PBA-a/BST composites as a function of BST ceramic loading measured at 1 MHz – 1 GHz.

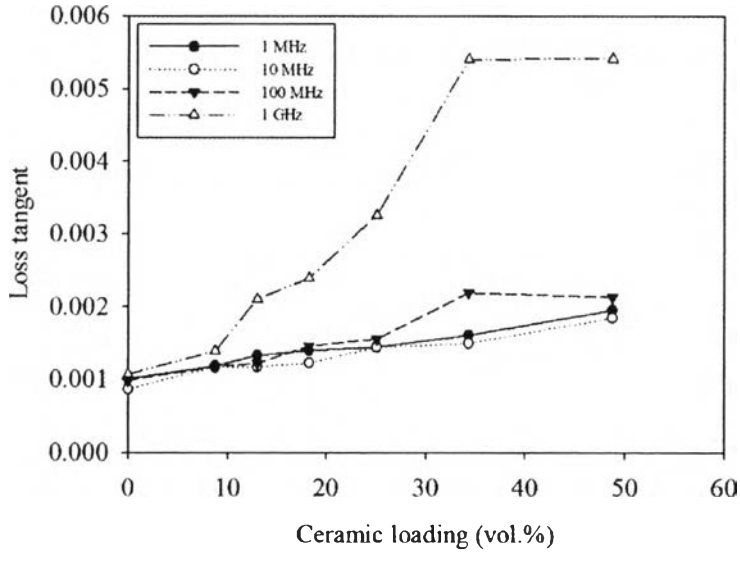

Figure 4.23 Loss tangent of the PBA-a/BST composites as a function of BST ceramic loading measured at 1 MHz – 1 GHz.

4.4.5.2 Frequency dependence of microwave dielectric properties

The frequency dependence of the dielectric constant and loss tangent at room temperature for the PBA-a/BST composites are shown in Figure 4.24 and 4.25,respectively . It can be seen that at the same ceramic content, dielectric constant decrease when frequency increases and also show significant decrease in dielectric

constant from 100MHz – 1GHz frequency ranges because at higher frequency, the dipole orientation polarization is inactive and resulted to low total polarization of the composites. In case of loss tangent, loss tangent value greatly increased at 100 MHz to 1 GHz which is the effect of polarity of polymer matrix [13].

4.4.5.3 Temperature dependence of microwave dielectric properties

For the effect of temperature to dielectric constant at 1 MHz and 1 GHz as shown in Figure 4.26 (a), (b), respectively. It was found that the higher temperature is resulting to the ability of molecule aliment slightly decreased leading to lower dipole orientation and decrease in dielectric constant. But this phenomenon was observed at 1 MHz to 100 MHz (for the graph of 10MHz and 100 MHz was not shown in here). At 1 GHz, the dielectric constant was constant with the temperature that means the composites have very low temperature coefficient which is the attractive requirement for microwave substrate application. While, the effect of temperature to loss tangent at 1 GHz as shown in Figure 4.27 shows insignificant increase with temperature. These can infer that temperature ranges of -50°C to 150°C are not effect to the segmental mobility of the polymer chain.

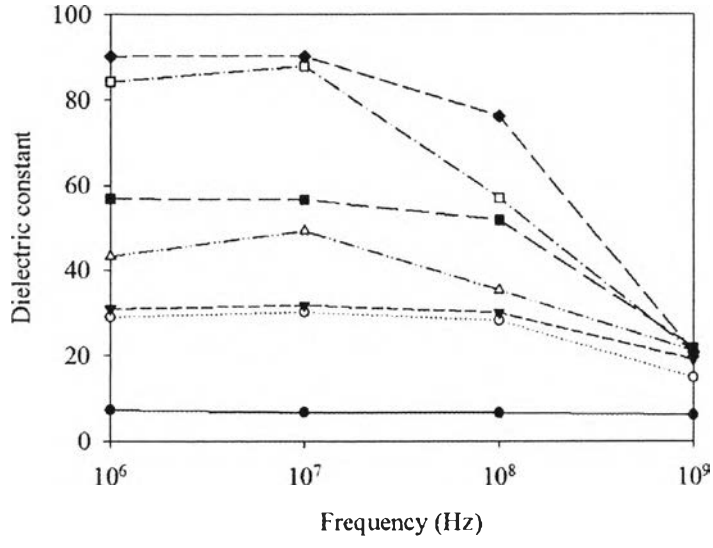

Figure 4.24 The frequency dependence of dielectric constant for PBA-a/BST composites at 1MHz – 1GHz

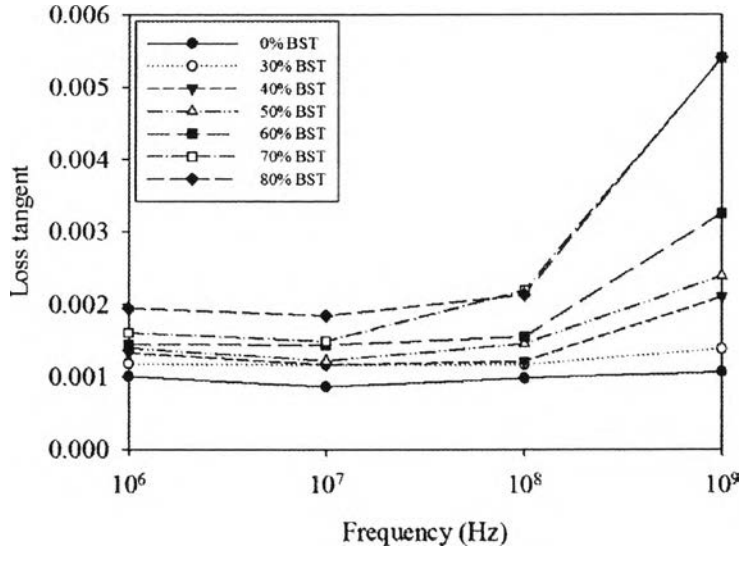

Figure 4.25 The frequency dependence of loss tangent for PBA-a/BST composites at 1MHz – 1GHz

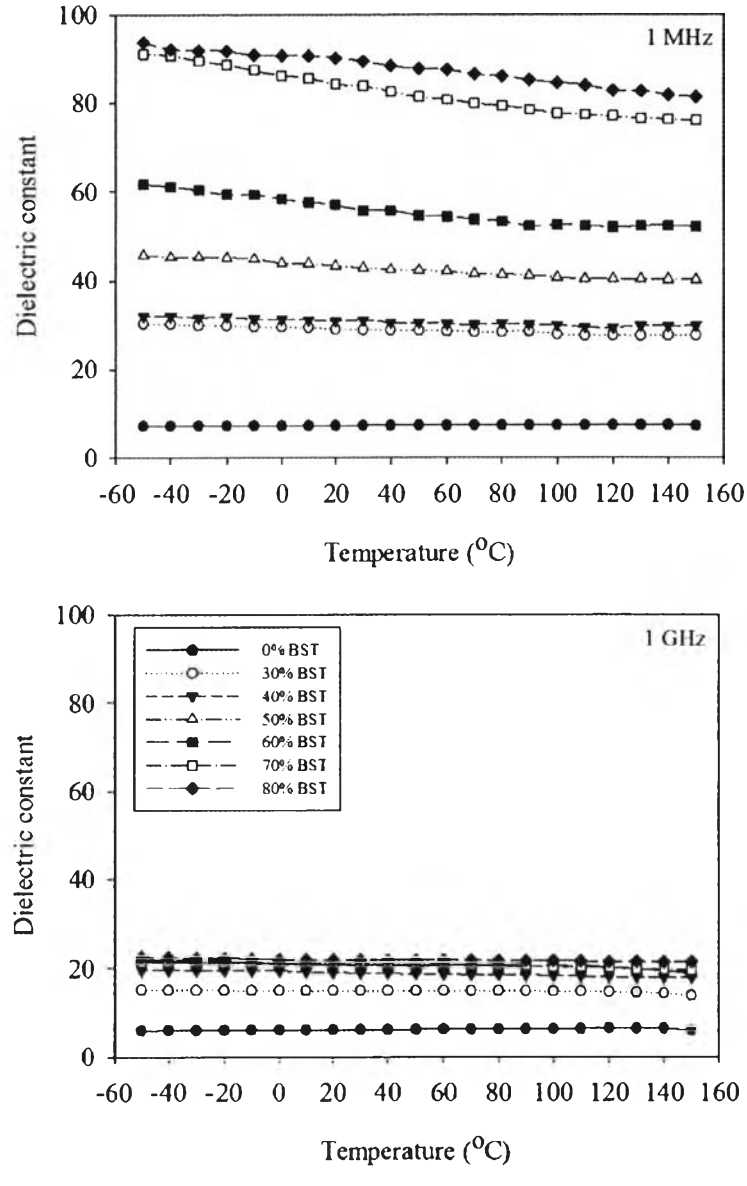

Figure 4.26 The temperature dependence of dielectric constant for PBA-a/BST composites at 1MHz (a) and 1GHz (b)

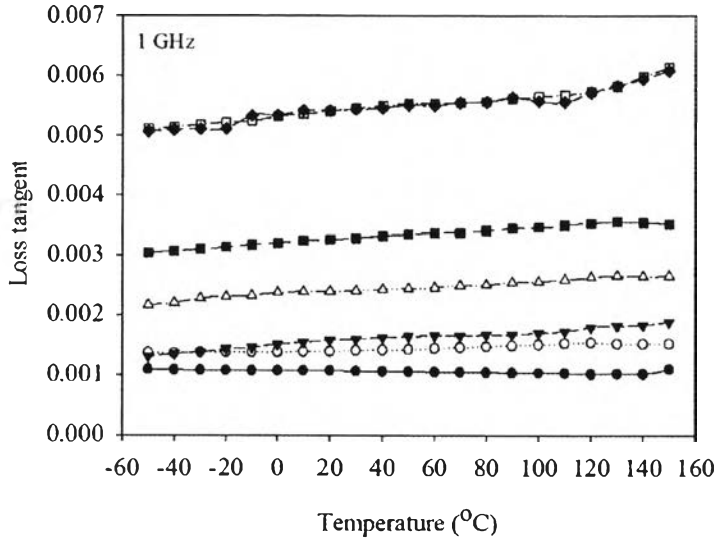

Figure 4.27 The temperature dependence of loss tangent for PBA-a/BST composites at 1GHz.

4.4.5.4 Experimental Data Fitting

There are many theoretical models have been proposed and used for predicting the dielectric constant of the polymer-ceramic composite comparing with the experimental results. The models that widely used such as series, parallel, Lichtenecker model, Bruggeman model and Kerner expression modified by Jayasundere-Smith (J-S prediction), as shown in Figure 4.28. The equations of these models are decribed as follow:

Series model $$\frac{1}{\varepsilon} = \frac{\phi_c}{\varepsilon_c} + \frac{\phi_p}{\varepsilon_p}$$

Parallel model $$\varepsilon = \phi_c \varepsilon_c + \phi_p \varepsilon_p$$

Lichtenecker model $$\log \varepsilon = \log \varepsilon_p + \phi_c \log \left(\frac{\varepsilon_c}{\varepsilon}\right)$$

Bruggeman formulae $$\frac{\varepsilon_c - \varepsilon}{\varepsilon_c - \varepsilon_p}\left(\frac{\varepsilon_p}{\varepsilon}\right)^{1/3} = 1 - \phi_c$$

Kerner expression $$\varepsilon = \frac{\varepsilon_p \phi_p + \varepsilon_c \phi_c [3\varepsilon_p/(\varepsilon_c + 2\varepsilon_p)][1 + 3\phi_c(\varepsilon_c - \varepsilon_p)/(\varepsilon_c + 2\varepsilon_p)]}{\phi_p + \phi_p (3\varepsilon_c)/(\varepsilon_p + 2\varepsilon_c)[1 + 3\phi_c(\varepsilon_c - \varepsilon_p)/(\varepsilon_c + 2\varepsilon_p)]}$$

where ε is the dielectric constant of the composites; ε_p and ε_c refer to the dielectric constants of the polymer matrix and the BST ceramic, respectively; ϕ_c and ϕ_p are the volume fraction of the ceramic and polymer, respectively[14].

From the comparison between the experimental data and five theoretical models, as indicated in Figure 4.28, It was found that the measured dielectric constant of the PBA-a/BST composites are higher than those calculated from series, parallel Lichtenecker model and J-S prediction model. It is noted that the measured dielectric constants show the tendency to fit well with Bruggeman model. It considers the composite as random mixture of nearly rough spherical inclusions.

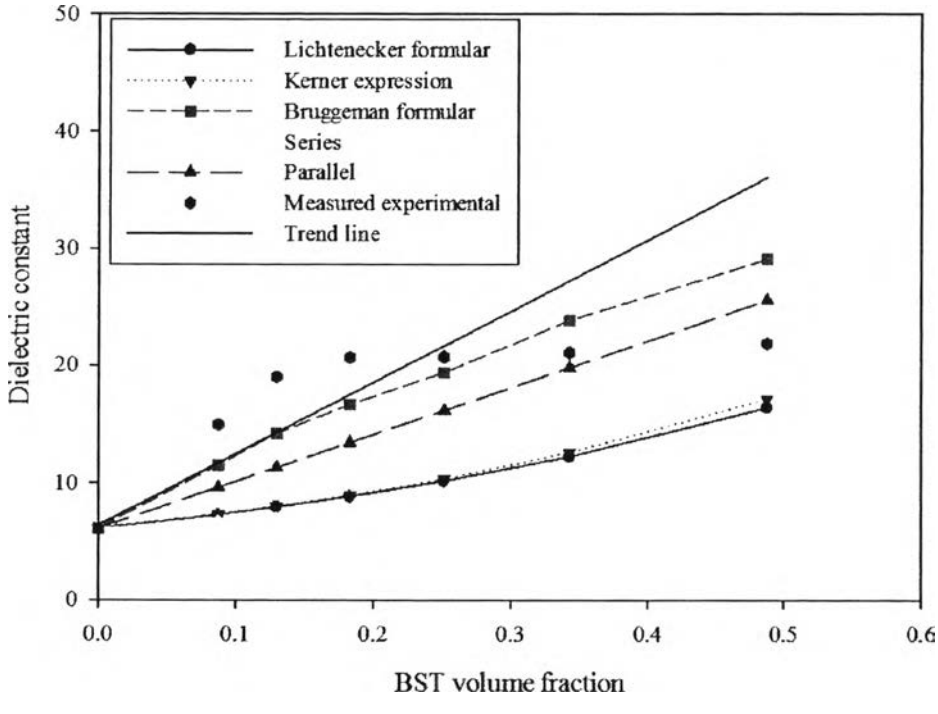

Figure 4.28 Plot of theoretical models and the measured dielectric constant for different BST volume fractions at room temperature and 1 GHz.

4.5 Conclusions

Aniline based polybenzoxazine was used as the polymer matrix for the composites because higher dielectric constants than those of fluorine based polybenzoxazine (6.12 and 4.49, respectively) along with the low loss tangent. The main reasons for lower dielectric constant of the fluorine based polybenzoxazine are the $-CF_3$ group which is the strong electron-withdrawing group so it shows the inductive effect and decreases the electronic polarizability moreover, bulky $-CF_3$ group lead to increase the free volume (ε_r of air near zero) and lastly, the lower polarizability of C–F bond can induce the hydrophobicity of the polymer. At higher frequency, the dipole orientation polarizability in the polymer molecule was decreased that leads to dielectric constant decrease. While at high temperature (150°C), the same effect was observed. For the PBA-a/BST composites, it was found that the dielectric constant can increase by the higher ceramic content. By adding 80 wt% (49 vol%) of BST powder, the dielectric constant increase from 6.12 to 22 at 1GHz. At higher frequency, the dielectric constants decrease resulted by the lower dipole orientation polarizability. At microwave frequencies, the composites show temperature independent dielectric properties. The PBA-a/BST composites could fit well with the Bruggeman model considering the composite as random mixture of nearly rough spherical inclusions. The composites in this work also show the improvement in thermal stability and stiffness properties which can observe from the higher decomposition temperature and glass transition temperature.

4.6 Acknowledgements

The authors thank the partial scholarship and partial funding of the research work provided by the Petroleum and Petrochemical College, Chulalongkorn University and Center of Excellence on Petrochemical and Materials Technology (PETRO-MAT) and the 90th Anniversary of Chulalongkorn University Fund (through the Ratchadaphiseksomphot Fund).

4.7 References

[1] Xu, J., and Wong, C.P. (2006). Effect of the polymer matrices on the dielectric behavior of a percolative high-k polymer composite for embedded capacitor applications. Journal of Electronic Materials, 35(5), 1087-1092.

[2] Zhi-Min Dang, Z.M., Yu, Y.F., Xu, H.P., and Bai, J. (2008). Study on microstructure and dielectric property of the BaTiO3/epoxy resin composites. Composites Science and Technology, 68, 171-177.

[3] Hu, T., Juuti, J., and Jantunen, H. (2007). RF properties of BST–PPS composites. Journal of the European Ceramic Society, 27, 2923-2926.

[4] Nisa, V.S., Rajesh, S., Murali, K.P., Priyadarsini, V., Potty, S.N., and Ratheesh, R. (2008). Preparation, characterization and dielectric properties of temperature stable SrTiO3/PEEK composites for microwave substrate applications. Composites Science and Technology, 68, 106-112.

[5] Sonoda, K., Juuti, J., Moriya, Y., and Jantunen, H. (2010). Modification of the dielectric properties of 0–3 ceramic–polymer composites by introducing surface active agents onto the ceramic filler surface. Composite Structures,92, 1052-1058.

[7] Kim, H.D., and Isida, H. (2002). Study on the chemical stability of benzoxazine-based phenolic resins in carboxylic acids. Journal of Physical Chemistry A, 106, 3217.

[8] Kumar, K.S.S., Nair, C.P.R., Radhakrishnan, T.S., ninan, K.N. (2007). Bis allyl benzoxazine: Systhesis, polymerization and polymer properties. European Polymer Journal, 43, 4504-2514.

[9] Su, Y.Ch., and Chang F.Ch. (2003). Synthesis and characterization of fluorinated polybenzoxazine material with low dielectric constant. Polymer, 44, 7989–7996.

[10] Zhang, J., Zhang, H., Lu, S.G., Xu, Z., and Chen, K.J. (2008). The effect of physical design parameters on the RF and microwave performance of the BST thin film planar interdigitated varactors. Sensors and Actuators A, 141, 231-237.

[11] Viswanath, R.N., and Ramasamy, S. (1997). Preparation and ferroelectric phase

transition studies of nanocrystalline $BaTiO_3$. Nano Structure Materials, 8(2), 155-162, 1997.

[12] Rimdusit, S., and Ishida, H. (2000). Development of new class of electronic packaging materials based on ternary systems of benzoxazine, epoxy, and phenolic resins. Polymer, 41, 7941-7949.

[13] Popielarz, R., Chiang, C.K., Nozaki, R., and Obrzut, J. (2001). Dielectric properties of polymer/ferroelectric ceramic composites from 100 Hz to 10 GHz. Macromolecules, 34, 5910-5915.

[14] Manuspiya, H., and Ishida, H. (2011). Polybenzoxazine based composites for increased dielectric constant. Polybenzoxazine Applications and Potential Applications, chapter 36, 621-639.